Thermodynamic Modeling of Arsenic in Copper Smelting Processes

CHUNLIN CHEN, LING ZHANG, and SHARIF JAHANSHAHI

Published data on the activity coefficients of arsenic in liquid copper, matte and, slag have been reviewed, assessed, and used in the development of thermodynamic databases for solution models of melts. The databases were validated against the literature data on the equilibrium distribution of arsenic between the matte and the slag. The models and databases were used in investigating the effects of matte grade, slag chemistry, SO_2 partial pressure, arsenic loading, and temperature on the equilibrium distribution of arsenic between the melts and gas phase during copper smelting and converting. The results obtained show that the continuous smelting processes operates close to equilibrium between condensed phases with most arsenic reporting to the gas phase. A comparison of the batch and continuous converting processes showed a considerable difference with respect to the elimination of the arsenic from condensed phases. These results indicate batch processes to be more efficient in the removal of arsenic through the gas stream.

DOI: 10.1007/s11663-010-9431-z

I. INTRODUCTION

INDUSTRY interest is growing in the deportment of arsenic (As) between various phases during the processing of base metal concentrates. This interest is driven by the gradual depletion of high-grade ore with low levels of impurities such as As, the requirements to manage the emission of toxic elements to the biosphere, and a growing need to produce high-purity salable products. Current knowledge and understanding of the factors affecting the deportment of arsenic between phases during concentrate smelting, matte converting, and copper refining are limited, dispersed in literature, and often incoherent to allow the development of optimum practices readily for the efficient removal and safe disposal of arsenic. Thermodynamic modeling, based on equilibrium calculation, has been used to simulate the minor elements distribution behavior in the copper smelting process through several studies.[1–4] In these studies, the system equilibrium is calculated by using the equilibrium constant method, in which the required activity coefficient equations or the equilibrium distribution ratio of components basically are derived from the experimental data on simple systems. An issue with this approach results from the extrapolation of the empirical equation(s) of the component's activity coefficient or distribution ratio from simple systems to complex industrial high-order systems. The second issue to consider is the possible departure from equilibrium in industrial processes and the effects of some process variables on the degree of disequilibrium in such processes. The present work was initiated with these issues in mind and was aimed at the development of enabling tools to analyze reactions taking place in smelting and converting processes, with ongoing work focusing on factors affecting the kinetics of reactions in smelting processes.

Since the early 1990s, the Commonwealth Scientific and Industrial Research Organisation (CSIRO) has been developing a thermodynamic modeling package called Multi-Phase Equilibrium (MPE) software using the CALPHAD method[5] for the calculation of multiphase equilibrium in metallurgical systems. This software has been applied successfully in the design and/or optimization of various smelting and metal-refining processes.[6,7] A broad range of oxide components, such as SiO_2, Al_2O_3, Cr_2O_3, TiO_2, Ti_2O_3, Fe_2O_3, FeO, CaO, MgO, MnO, CrO, PbO, NiO, CoO, ZnO, Na_2O, and Cu_2O have been included in its slag and solid solution databases. One of the recent developments has been to extend the MPE model capability to cover the behavior of minor elements, such as arsenic, antimony *etc*. and to use this software to analyze the behavior of minor elements under practical/industrial conditions. For this purpose, the thermodynamic behavior of minor elements such as As in matte, slag, and liquid copper phases were reviewed critically, and the results were used in developing optimized databases for the solution models. More details on the MPE software and its capability have been presented elsewhere.[6–9]

In the present study, the modeling results of As in liquid copper, slag, and matte are presented and discussed. Validation of the developed databases against published data on the distribution of As between slag and matte phases also is presented. Published data on the deportment of As between phases in commercial flash and bath smelting processes are compared with the

CHUNLIN CHEN, Senior Research Scientist, LING ZHANG, Principal Research Scientist, and SHARIF JAHANSHAHI, Theme Leader-Sustainable Processing, are with CSIRO Minerals Down Under National Research Flagship, Clayton South, VIC 3169, Australia. Contact e-mail: chunlin.chen@csiro.au.

Manuscript submitted July 2, 2009.
Article published online September 8, 2010.

calculated equilibrium values, and the initial analysis of the degree of disequilibrium in such processes is presented. Finally, the effects of the matte grade, SO_2 partial pressure, slag chemistry, and temperature on the deportments of As in copper smelting and converting processes were studied and are discussed.

II. MODEL DEVELOPMENT

A. *Solution Models*

The Redlich-Kister-Muggianu polynomial[10] was used to describe the excess Gibbs energy of the molten copper phase and is depicted as follows:

$$G_m^{ex} = \sum_i \sum_{i<j} x_i x_j \sum_v L_{ij}^v (x_i - x_j)^v \qquad [1]$$

where L_{ij}^v is the interaction coefficient components i and j.

The cell model developed by Gaye and Welfringer[11] was used for the liquid slag. The model is a statistical thermodynamic model based on the description of liquids in terms of cells that consist of a certain anion surrounded by two cations. The free energy of mixing for the system then is associated with the following energy parameters: Wij, which is the energy associated with the formation of an asymmetric cell from two symmetric cells, and Eij, which is the energy associated with the interaction between a symmetric and an asymmetric cell.

The modified quasichemical model for short-range ordering has been developed successfully to describe the matte phase by Kongoli *et al.*[12,13] This model was extended to cover the arsenic in the matte by introducing the cation–arsenic interactions and the arsenic–sulfur interactions in the present study.

B. *Thermodynamic Data*

The Gibbs free energy data of solid and liquid arsenic, arsenic gas species, as well as the As_2O_3 are necessary for calculating the deportment of arsenic among the gas, matte, and slag phases during the smelting process. The selected thermodynamic data for As species are listed in Table I.

Table I. Selected Gibbs Free Energy Data for Arsenides

Reaction	ΔG^o (J/mole)	Source
As (s,α) = As (l)	22433 − 11.51 T-1.30 TlnT	[14]
As (l) = As (g)	257,700 – 109.09 T	[14]
2As (l) = As_2 (g)	122,880 – 103.86 T	[14]
3As (l) = As_3 (g)	154,526 – 113.45 T	[14]
As (l) = As_4 (g)	37,560 – 64.38 T	[14]
0.5As_2 (g) + 0.5S_2 (g) = AsS (g)	18,200.4 – 11.13 T	[15]
0.5As_2 (g) + 0.5O_2 (g) = AsO (g)	–39,999 – 11.59 T	[16]
As_2 (g) + 1.5O_2 (g) = As_2O_3 (s)	–819,589 + 373.99 T	[17]
As_2O_3 (s) = As_2O_3 (l)	18,000 – 30.66 T	[17]

C. *Arsenic in the Liquid Copper*

The experimental data on the Cu-As system was reported in several studies[18–22] over a temperature range of 1273 K to 1423 K (1000 °C to 1150 °C). The data on the activity of arsenic in liquid copper from these studies[18–22] were reviewed and reevaluated critically using more accurate thermodynamic data for arsenic vapor species by Pei.[23] The arsenic activity reported by Bode *et al.*[18] was not considered to be accurate, as their reported results neglected the contribution of the vapor pressure of copper, which could be much higher than the total pressure of arsenic species in equilibrium with low arsenic copper alloys. As shown in Figure 1, the experimental data from References 19 through 22 after Pei's reassessment show good agreement. In the present study, these data, which were unified by Pei,[23] were used to optimize the model parameters for describing the As in liquid Cu. The optimized model parameters are given in Table II. A comparison of the calculated γ_{As} using the liquid standard state with the experimental data on the Cu-As system also is shown in Figure 1. It is evident that good agreement exists between the model's calculation and the experimental measurements over a broad range of concentration with some orders of magnitude variation in the γ_{As} when the activity coefficient at infinite

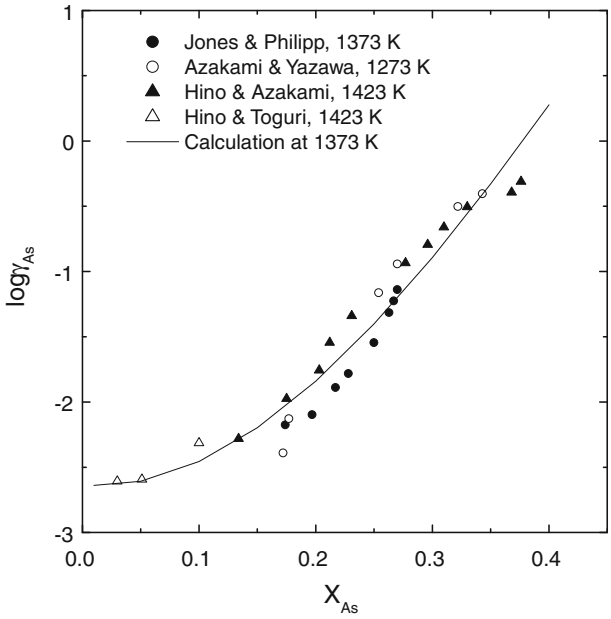

Fig. 1—The comparison of the calculated activity coefficients of As in the liquid copper to that of the measured,[23] material relative to pure liquid arsenic as a standard state.

Table II. Optimized Model Parameters of As in Molten Copper

$L^0_{Cu-As} = -47{,}872.33$
$L^1_{Cu-As} = 68{,}370.3$
$L^2_{Cu-As} = 1185.4$
$L^3_{Cu-As} = -47{,}573.6$

dilution (γ^0_{As}) was set to 0.004 at 1523 K (1250 °C). It is worth noting that when lower values for γ^0_{As} are used (*e.g.*, 0.0007 at 1523 K [1250 °C] as has been used in References 3 and 4), a significant underestimation of the arsenic removal during copper smelting results.

D. *Arsenic in the Slag*

In the published modeling studies, the As was modeled in a different form in the slag by different researchers. The As in the slag was modeled as an element by Nagamori and Chaubal,[1] as AsO_4^{3-} by Reddy and Font,[24] and as $AsO_{1.5}$ by Itagaki and Yazawa,[2] Kim and Sohn,[3] and Tan and Zhang.[4] As discussed in our accompanying article,[25] the trivalent oxide of As (As^{3+} or $AsO_{1.5}$) is expected to be present in calcium ferrite and iron silicates slags over the oxygen potential rage of 10^{-9} to 10^{-7} atm, which are practiced commonly for copper smelting and converting. The $\gamma_{AsO_{1.5}}$ in the calcium ferrite slag from the previous study agrees well with that of Takeda *et al.*[26] However, the values of $\gamma_{AsO_{1.5}}$ in iron silicate slag obtained from our study[25] differ from these reported by Takeda *et al.*,[26] which were derived from study by Kashima *et al.*[27] To date the cause of this discrepancy has not been identified. The consistency between the $\gamma_{AsO_{1.5}}$ in the iron silicate slag from the current study and in the calcium ferrite slag was confirmed by the equilibrium distribution ratio of arsenic among the iron silicate slag, the calcium ferrite slag, and the copper matte measured by Roghani *et al.*[28] Therefore, the data from Kashima *et al.*[27] is inconsistent with other studies and was not used in our assessment. The $\gamma_{AsO_{1.5}}$ measured through our previous study[25] as well as those in the calcium ferrite slag by Takeda *et al.*[26] were used for optimizing model parameters for $AsO_{1.5}$ in slags, which are listed in Table III. It is evident from Figure 2 that the agreement between the experimental and the calculated values of $\gamma_{AsO_{1.5}}$ is good and that the model represents variation in the behavior of arsenic over a range of slag chemistry as well as over several orders of magnitude in oxygen potential. The estimated activity coefficient of $AsO_{1.5}$ in the silica-saturated iron silicate slag (the dotted line in Figure 2) needs to be confirmed by further experimental investigation.

E. *Arsenic in the Matte*

The thermodynamic behavior of arsenic in Cu-S and Cu-Fe-S mattes has been measured by numerous investigators.[22,29–35] The distribution ratio of arsenic between liquid copper and Cu_2S melts was measured by Asano and Wada,[29] Nagamori *et al.*,[30] Hino and Toguri,[22] and Mendoza *et al.*[31] Generally, the agreement between these studies[22,29–31] is good with the reported As distribution ratio being about 10 at temperatures between 1423 K and 1473 K (1150 °C and 1200 °C). Itagaki *et al.*[32] measured the activity of arsenic in mattes along the Cu_2S-FeS pseudobinary system containing 16 to 60 wt pct copper at 1373 K (1100 °C), by using the isopiestic technique. They found that the activity coefficient of arsenic in the matte phase decreases remarkably by increasing the sum of the copper and iron activity. This behavior could be explained in terms of the strong chemical affinity copper and iron have for arsenic. Lau *et al.*[33] determined the As activity in a matte with the composition 35.0 wt pct Cu, 35.8 wt pct Fe, and 19.9 wt pct S at 1336 K (1063 °C) with the torsion-effusion method. The activity coefficient of arsenic in the matte had a value of 0.7 ± 0.2 in the composition range studied, which is about one order of magnitude lower than that of Itagaki *et al.*[32]

Roine and Jalkanen[34] used the transportation technique to determine the activity and activity coefficient of arsenic in Cu-Fe-S mattes with various Cu/Fe ratios and S-to-metal ratios at 1473 K (1200 °C). The sulfur-to-metal ratio, which controls the activities of Fe and Cu in the matte, was the most important factor that influenced the arsenic activity coefficient. At fixed Cu/Fe ratios, the As activity coefficient increased with an increasing S content in the matte. For the pseudobinary Cu_2S-FeS mattes, the γ_{As} reported by Roine and Jalkanen[34] seemed to agree with the data of Itagaki *et al.*[32] One obvious drawback in the experiments by Roine and Jalkanen is the vaporization of As during the heating and cooling of samples. The heating and cooling period was about 45 minutes, which was not accounted for, and all As lost from the sample was assumed to have

Table III. Optimized Model Parameters of As in Slag*

$W^0_{SiO_2-As_2O_3} = 10{,}652$; $E^0_{SiO_2-As_2O_3} = 5573$
$W^0_{As_2O_3-Fe_2O_3} = 168{,}242$; $E^0_{As_2O_3-Fe_2O_3} = 2582$
$W^0_{As_2O_3-CaO} = -261{,}390$; $E^0_{As_2O_3-CaO} = -89.2$
$W^0_{As_2O_3-MgO} = -3307$
$W^0_{As_2O_3-FeO} = -95{,}463$; $E^0_{As_2O_3-FeO} = -47$

*The cell model parameters are defined in Ref. 11.

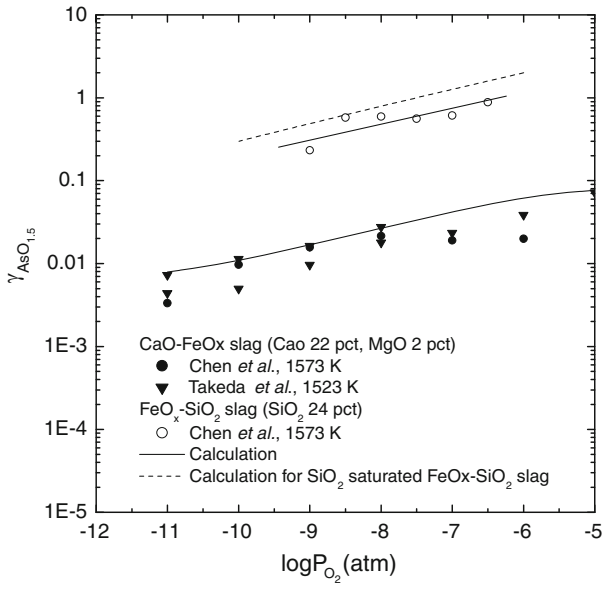

Fig. 2—Comparison of the calculated activity coefficients of $AsO_{1.5}$ in the slag ($\gamma_{AsO_{1.5}}$) to that of measured values by Chen and Jahanshahi[25] and Takeda *et al.*[26]

resulted from vaporization during the bubbling/blowing period, which is about 30 to 60 minutes for most of their experiments. It thus is thought that the drawback of their experimental procedure could have caused the overestimation of γ_{As} in their mattes. The transportation technique used by Roine and Jalkanen[34] was modified by Zhong and Lynch[35] to overcome the previously mentioned drawback and was used to evaluate the Henrian activity coefficient of As in Cu-Fe mattes and white metal (Cu_2S) at 1493 K and 1533 K (1220 °C and 1260 °C). Zhong and Lynch found that γ^0_{As} is strongly dependent on the As content, even at trace concentrations when Henrian behavior is expected. These authors attributed this dependency to the uncertainty in the reported value of the saturation pressure of monoatomic arsenic (P^0_{As}). To reduce the impact of P^0_{As}, the activity coefficient of arsenic was calculated at an arsenic concentration in which diatomic arsenic is the dominant elemental vapor species and in which the P_{As} over the melt accounts for only 1 wt pct of P_{As_2}.

Hino and Toguri[22] and Mendoza *et al.*[31] used the Knudsen cell-mass spectrometric method to measure the activity of arsenic at low arsenic contents in the miscibility gap of molten Cu-Fe-S mattes at 1473 K (1200 °C). The measured activity coefficients of arsenic from these two studies show good agreement with each other and demonstrate a negative deviation from Raoult's law. Furthermore, the measured activity coefficient of arsenic (γ_{As}) showed a strong dependence on the concentration of As in mattes. Extrapolation of these results to an infinitely dilute solution of As in Cu-S and Cu-Fe-S mattes indicates that the value of γ^0_{As} approaches 0.055 at 1473 K (1200 °C).

It is worth noting that the Gibbs energy data for the gaseous arsenic species and AsS used in References 22, 31, 32, and 35 for calculating the γ_{As} disagree with each other, which complicates the comparison of values of γ_{As} between studies. As demonstrated by Pei[23] through his assessment of arsenic activity in liquid copper, the thermodynamic data for condensed arsenic and arsenic vapor species as assessed by Gokcen[14] is believed to be the most accurate, and the apparent discrepancies between different studies could be resolved readily through the use of unified thermochemistrty data. Thus, in the present study, the activity coefficient of As in the matte from References 22, 31, and 32 was recalculated using the Gokcen's data[14] and are presented in Figure 3.

Given the uncertainties in some of these studies,[33,34] it was decided to use the data by Hino and Toguri,[22] Mendoza *et al.*,[31] Itagaki *et al.*[32] and Zhong and Lynch[35] to optimize the model parameters for As in the matte. The model parameters are listed in Table IV. As shown in Figure 3, the variation of the As activity coefficient γ_{As} with the matte grade is represented reasonably by the model.

III. MODEL VALIDATION

To assess the compatibility of the developed solution models/databases for the behavior of arsenic in liquid copper, matte, and slag phases and hence to validate the

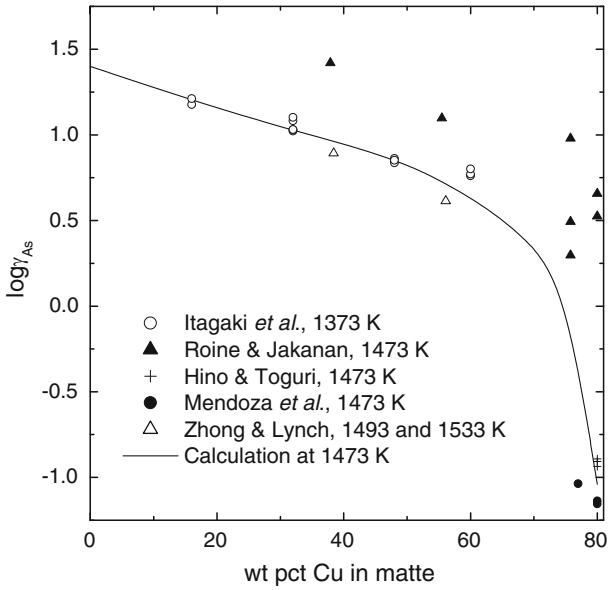

Fig. 3—Comparison of the calculated activity coefficients of As in the matte (γ_{As}) with those measured by Mendoza *et al.*,[31] Itagaki *et al.*,[32] Roine and Jakanan,[34] and Zhong and Lynch.[35]

Table IV. Optimized Model Parameters of As in Matte*

$Z_{As} = 2.75$
$\omega^0_{As,S} = 232{,}073; \omega^1_{As,S} = 69.16; \omega^6_{As,S} = -1782.8$
$\omega^0_{Cu,As} = -83{,}851.4; \omega^1_{Cu,As} = -1719.2; \omega^3_{Cu,As} = 893{,}699$
$\omega^0_{Fe,As} = -54{,}107; \omega^0_{Fe,As} = -1696.9$

*The quasichemical matte model parameters are defined in Ref. 12.

MPE software, some comparison of the measured and calculated data on the equilibrium distribution of As between the slag and the matte will be presented in this section. Laboratory experimental data on both iron silicate and calcium-ferrite-based slags will be covered.

A. *Iron Silicate Slag and Matte Equilibrium*

Yazawa *et al.*[36] measured the equilibrium distribution ratio as defined in Eq. [2] of As between silica-saturated iron silicate slags and copper mattes at 1573 K (1300 °C) under a flow of SO_2 at 0.1 atm partial pressure. Johnson *et al.*[37] also investigated the distribution of As between the copper matte and the silica-saturated iron silicate slag, but it was studied at 1523 K (1250 °C) and under controlled gas atmospheres comprising CO, CO_2, and 10 pct SO_2. Roghani *et al.*[28] reported the distribution ratio of As between silica-saturated iron silicate-based slags containing 5 to 10 wt pct MgO at 1573 K (1300 °C) under varied SO_2 partial pressures. Equation [2] is expressed as follows:

$$L^{slag/matte}_{As} = \frac{(\text{wt pct As in slag})}{(\text{wt pct As in matte})} \qquad [2]$$

Figure 4 shows the variation of $L^{slag/matte}_{As}$ with the matte grade reported by Yazawa *et al.*,[36] Johnson *et al.*,[37]

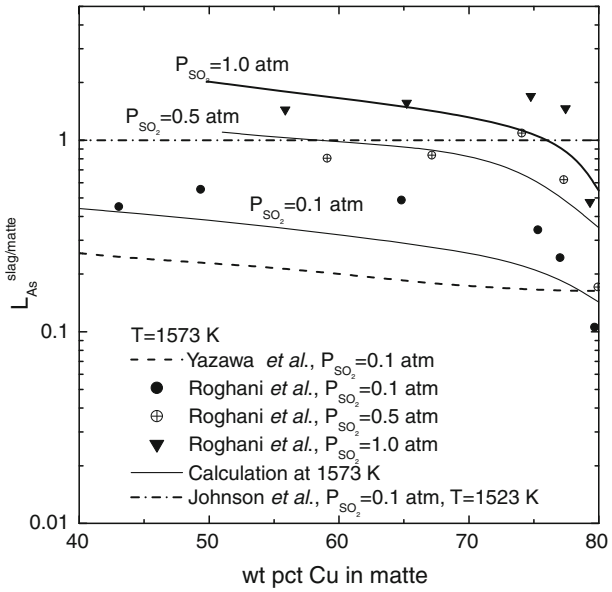

Fig. 4—Comparison of the calculated distribution of As between the iron silicate slag and the matte ($L_{As}^{slag/matte}$) with measured values by Roghani *et al.*,[28] Yazawa *et al.*,[36] and Johnson *et al.*[37]

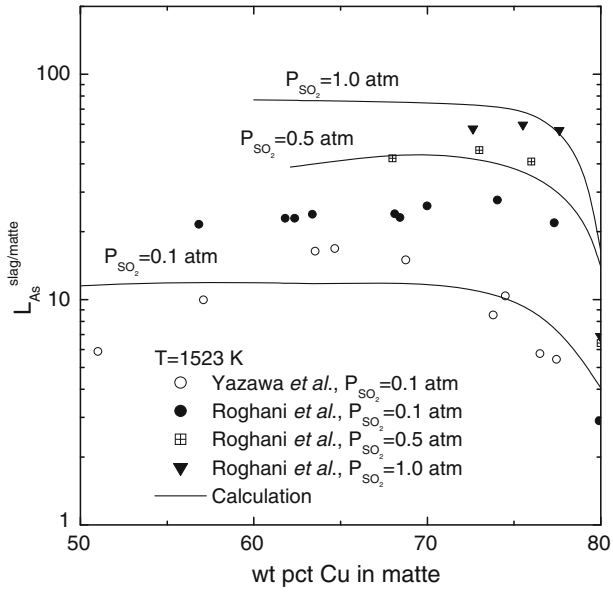

Fig. 5—Comparison of the calculated distribution of As between the calcium ferrite slag and the matte ($L_{As}^{slag/matte}$) with measured values by Acuna and Yazawa,[39] and Roghani *et al.*[40]

and Roghani *et al.*[28] The values of $L_{As}^{slag/matte}$ obtained by Roghani *et al.* at P_{SO_2} of 0.1 atm lay between those reported by Yazawa *et al.* and Johnson *et al.* at the same P_{SO_2}. The $L_{As}^{slag/matte}$ values from References 28 and 37 under 0.1 atm SO_2 are close to each other but are slightly higher than those of Yazawa *et al.*[36] Both Roghani *et al.* and Yazawa *et al.* reported decreases in the distribution ratio of $L_{As}^{slag/matte}$ as the matte grade increases. According to Roghani's data, a sharp decrease in the $L_{As}^{slag/matte}$ occurs as the matte grade increases beyond 70 wt pct of Cu. In Roghani's study,[28] $L_{As}^{slag/matte}$ increased with an increasing SO_2 partial pressure at fixed Cu grades because of the increase in oxygen partial pressure with an increasing SO_2 partial pressure at a given matte grade and because of the effect of a higher oxygen partial pressure on the oxidation of As into the slag. As shown in Figure 4, the effects of the matte grade as well as the SO_2 partial pressure on the distribution of As between silica-saturated iron silicate slag and Cu matte at 1573 K (1300 °C) from the experimental measurements can be represented by the MPE software.

B. *Calcium Ferrite Slag and Matte Equilibrium*

Compared with the conventional iron silicate slag, calcium ferrite slag has the benefits of a low solubility of copper and a low viscosity, which result in lower copper losses to the slag through chemical and mechanical entrainment, respectively. The calcium-ferrite-based slag has been used commercially in the Mitsubishi copper-converting process.[38] The distribution of As between the matte and the calcium ferrite slags at 1523 K (1250 °C) under 0.1 atm SO_2 first was investigated by Acuna and Yazawa.[39] Roghani *et al.*[40] also reported the distribution ratio of As between the calcium ferrite slag and the copper matte at 1523 K (1250 °C) under varied SO_2 partial pressures. The $L_{As}^{slag/matte}$ values for calcium ferrite slags reported by Acuna and Yazawa[39] and by Roghani *et al.*[40] under 0.1 atm of SO_2 are close. As shown in Figure 5, the $L_{As}^{slag/matte}$ increases slightly with the increasing matte grade until the Cu in the matte reaches 70 to 75 wt pct Cu. Beyond this point, $L_{As}^{slag/matte}$ starts to decrease as a result of the decrease of the activity coefficient of As in the matte. The $L_{As}^{slag/matte}$ value for calcium ferrite slags was about one order of magnitude higher than that for iron silicate slags. For the same reason mentioned in the previous section, $L_{As}^{slag/matte}$ increased with an increasing SO_2 partial pressure at fixed Cu grades in Roghani's work.[40] The calculated distributions of As between the calcium ferrite slags and the matte at 1523 K (1250 °C) under 0.1, 0.5, and 1.0 atm SO_2 are compared with the experimental data in Figure 5. Comparison of the experimental data with those from the model shows that the model makes a good prediction of the As distribution between calcium ferrite slags and the copper matte.

IV. MODEL APPLICATIONS IN PROCESS ANALYSIS

A. *Comparison of Plant Data*

The available data on As distribution between the matte and the slag from several commercial bath smelting[38,41,42] and flash smelting[43] processes are presented in Figure 6 as a function of matte grade. The scatter in each set of plant data includes some variations in the process variables that affect As partitioning and possible errors or uncertainties in the determination of low levels of As in the matte or the slag. Despite scatter in the plant data, the general trend

shows that the distribution ratio decreases with an increasing matte grade. This trend is consistent with measurements of the equilibrium distribution as shown in Figure 4 for iron silicate slags. The solid curve in Figure 6 is the calculated equilibrium distribution for the operating conditions employed in the smelting stage of the Noranda process (FeO_x-25 pct SiO_2, P_{SO_2} = 0.2 atm, and 1523 K [1250 °C]). It is evident from this plot that the plant data are mostly lower than the equilibrium curve, thus indicating that the matte and slag phases were approaching equilibrium from the matte phase in these processes. The slightly higher values of As distribution between the slag and the matte at equilibrium as calculated by MPE suggests that further improvements in As removal could be achieved by taking appropriate measures (*e.g.*, improve mixing between the condensed phases to enhance the mass transfer and to reduce the degree of disequilibrium between the phases). According to Figure 6, the distribution of As between the slag and the matte in the smelting stage of the Mitsubishi process is slightly lower than that in the Noranda, Outokumpo, and Isasmelt processes.[38,41–43] One key reason for this difference is the slag chemistry. The data on the Mitsubishi smelting process show that the slag is close to silica saturation, whereas the slags of the Noranda, Outokumpo, and Isasmelt processes contain about 25 wt pct SiO_2. As shown in Figure 2, the activity coefficient of $AsO_{1.5}$ in the iron silicate slags increases with an increase in the SiO_2 content of the slag. Therefore, the higher SiO_2 content of the Mitsubishi smelting slag decreases the arsenic capacity of the slag. However, the 5 wt pct CaO in the Mitsubishi smelting slag is expected to increase the arsenic capacity in the slag slightly, which only can offset the arsenic capacity decrease partially caused by a high amount of SiO_2 in slag. It is worth pointing out that other process variables, such as the intensity of mixing and the contact area between phases, also could influence the degree of departure from equilibrium; however, without data on such variables for the aforementioned processes, assigning the observed difference to the differences in the slag practice is tentative.

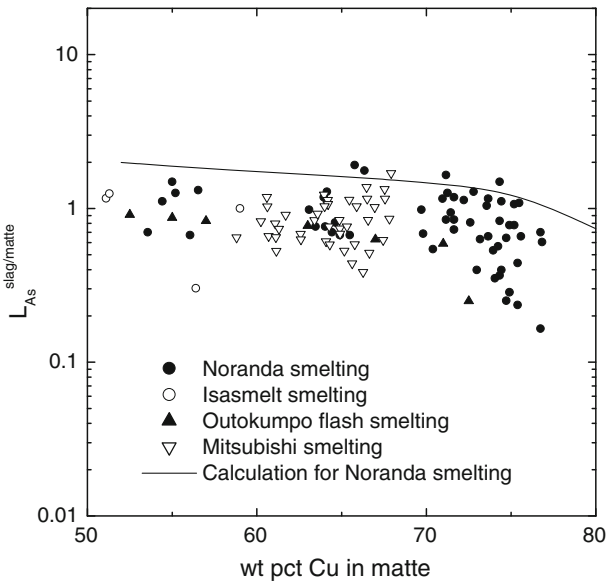

Fig. 6—Comparison of the calculated equilibrium distribution of As between the iron silicate slag and the matte ($L_{As}^{slag/matte}$) with published data from plant measurements.[38,41–43] The calculated equilibrium distribution ratio were for slags with an Fe/SiO_2 ratio of 2.2 at 1523 K (1250 °C) and P_{SO_2} of 0.2 atm.

The copper smelting processes can be classified into steady-state/continuous processes (*e.g.*, Mitsubishi and Isasmelt bath smelters[38,42] and Outokumpo flash smelter[43]) and batch-type processes (*e.g.*, Peirce-Smith converter).[44] In the continuous processes, the feed materials are charged continuously and smelted with molten products being tapped on a semicontinuous basis while the reacted gases leave the reactor continuously. As the process operates under a steady-state condition, it can be modeled with a one-step equilibrium calculation. However, for modeling the batch-type operations in which the feed materials are added at once rather than over the smelting cycle, the process should be divided into a series of short time steps to allow for removal of the reacted gas from the condensed phases at the end of each step. In this way, the variations of the system compositions and temperature with the gas injection period could be calculated. In the following sections, the results obtained from simulations of continuous and batch type processes, using the MPE software, will be presented and discussed briefly.

B. *Steady-State/Continuous Operation Modeling*

1. *Oxygen and sulfur partial pressure*

In copper smelting/converting, As is eliminated through oxidation into the slag and evaporation into the gas. The dominant As gas species is AsS. The oxygen and sulfur partial pressures are expected to have a strong effect on the As distribution. Figure 7 shows the calculated variations of the oxygen and sulfur partial pressures against the Cu grade at 1523 K (1250 °C) under 0.1

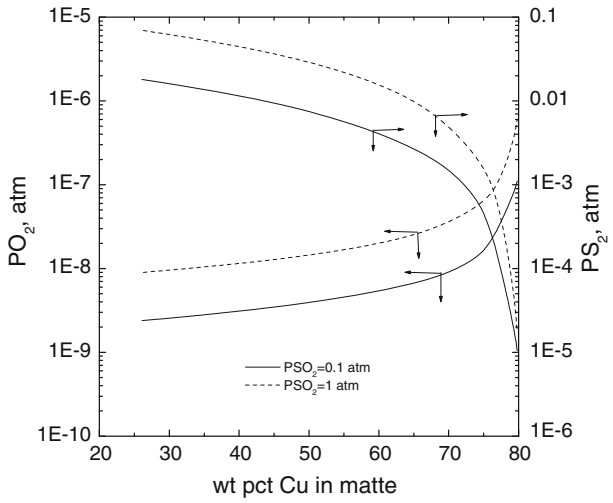

Fig. 7—Variations of oxygen and sulfur partial pressures under varied SO_2 partial pressure at 1523 K (1250 °C) *vs* matte grade.

and 1.0 atm SO_2 during copper smelting/converting with a silica-saturated iron silicate slag. The sulfur partial pressure decreases with an increasing matte grade, whereas the oxygen partial pressure increases. At a given matte grade, the oxygen and sulfur partial pressures increase with an increasing SO_2 partial pressure.

2. *Copper smelting (matte making)*

The effects of matte grade, slag chemistry, SO_2 partial pressure, temperature, and As concentration in the feed concentrate on the deportment of As to the gas, matte, and slag phases in copper smelting were examined with the help of the comprehensive slag, matte, and liquid copper databases developed. Note that the slag chemistry and the temperature vary from process to process. The iron silicate slag is used widely in most commercial copper smelting processes. This type of slag also contains low levels of Al_2O_3 and MgO, which originate from the concentrate and flux. To simplify the modeling, silica-saturated iron silicate slag was used as a base case of the smelting modeling. The operating conditions used in these calculations of the smelting process are listed in Table V and the results from the modeling are shown in Figures 8(a) to (f).

Table V. Basic Operation Conditions of the Smelting Process

Feed
Matte: 40 pct Cu_2S, 59.8 pct FeS, and 0.2 pct As
Silica flux: SiO_2 100 pct
Input air: 21 vol pct O_2
Slag chemistry: silica-saturated iron silicate slag
Temperature: 1523 K (1250 °C)

In Figure 8(a), the variations in the calculated equilibrium distribution of As among the gas, slag, and matte phases with the final matte grade at 1523 K (1250 °C) are presented. These results show that at low matte grades, more than 75 pct of the As reports to the gas phase with the balance being predominantly

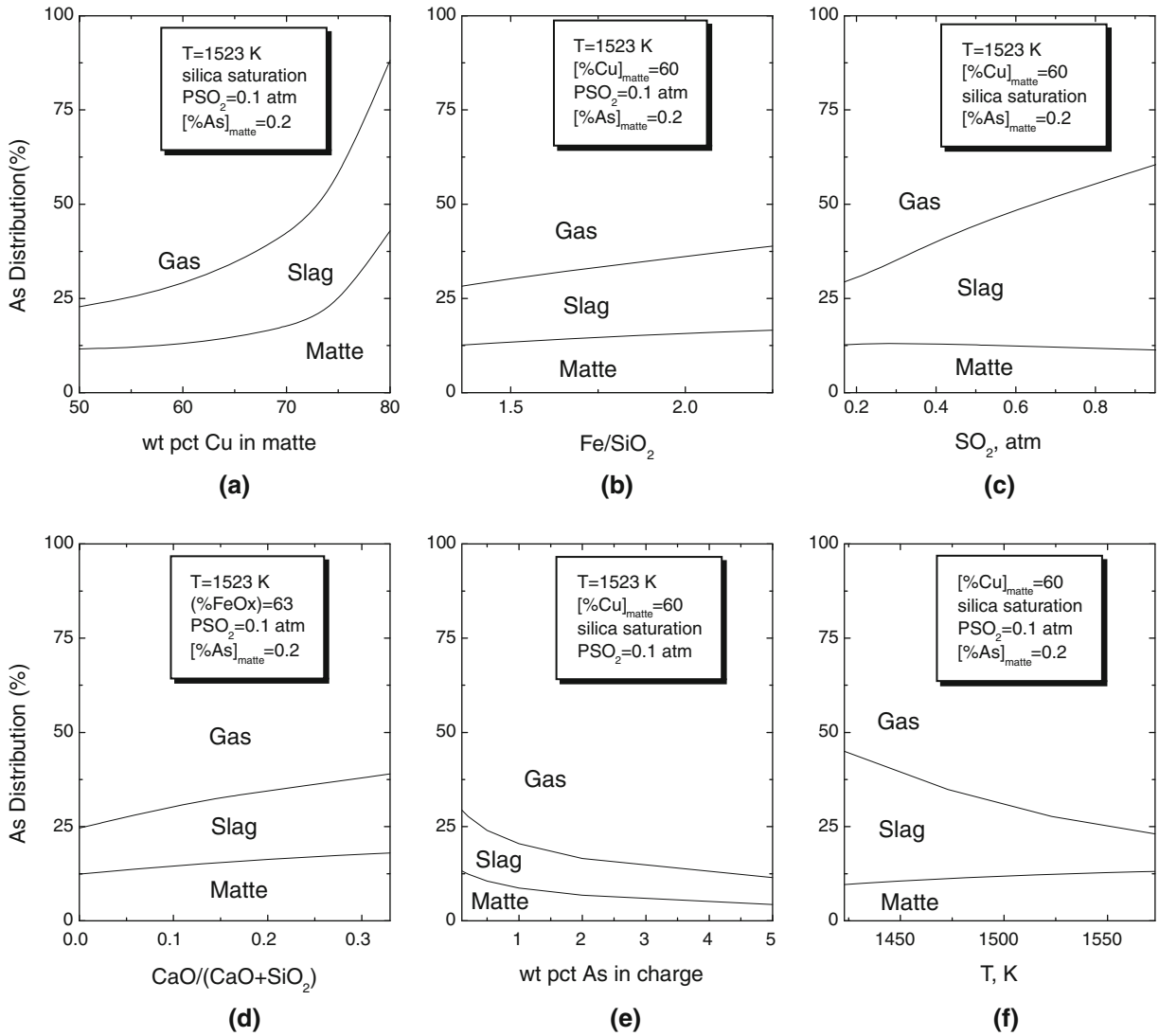

Fig. 8—The distribution of As among the gas, silica-saturated iron silicate slag, and copper matte phases during continuous smelting of charge matte (40 pct Cu_2S, 59.8 pct FeS, and 0.2 pct As) at 1523 K (1250 °C) with $P_{SO_2} = 0.1$ atm.

contained in the matte. However, as the matte grade increases, the relative portion of As that reports to the gas phase decreases to less than 15 pct at a matte grade of about 80 pct with marked increases in the deportment to the slag and matte phases. This apparent effect of matte grade is caused by multiple contributing factors that also are dependent on matte grade. As discussed in the previous section, the activity coefficient of As in the matte decreases with an increasing matte grade; thus, higher grade mattes have a higher affinity for arsenic and hence reduce the activity and vapor pressure of As. The activity of sulfur in mattes also decreases with increasing matte grade, thus causing lower partial pressures of S_2 and hence a lower degree of volatilization of As as AsS at higher matte grades. The other key factors to consider are the decrease in matte and the increase in slag masses as the matte is smelted to higher grades. Figure 4 shows that the distribution ratio between the slag and the matte ($L_{As}^{slag/matte}$) starts to decline sharply at matte grades greater than 70 pct. By taking into account the changes in mass of these phases and $L_{As}^{slag/matte}$, one could see how these contributing factors affect the deportment. According to the results shown in Figure 8(a), to maximize the deportment of As to the gas phase, the target matte grade for the smelting stage should be below 65 pct.

Figure 8(b) shows the calculated effect of the Fe/SiO_2 ratio on the distribution of As among the gas, slag, and matte at 1523 K (1250 °C) for a matte grade of 60 pct Cu and an SO_2 partial pressure of 0.1 atm. As is shown, the arsenic content of the slag is expected to increase from about 15 pct to 22 pct with an increasing Fe/SiO_2 ratio. As is explained in previous sections, the activity coefficient of $AsO_{1.5}$ in the silica-saturated iron silicate slag is slightly higher than that in the slag with 25 pct SiO_2. Therefore, increasing the Fe/SiO_2 ratio in the slag leads to a moderate decrease in the activity coefficient of $AsO_{1.5}$ in the slag, which results in raising the arsenic deportment to the slag phase. This effect of the Fe/SiO_2 ratio is also evident in plant data, which was discussed with reference to Figure 6.

During copper smelting, the SO_2 pressure can vary from 0.1 atm at the bath smelting process to more than 0.9 atm in flash smelting processes with the use of tonnage oxygen. The effect of SO_2 partial pressure on the distribution of As at 60 wt pct Cu grade was calculated at 1523 K (1250 °C) for a slag saturated with silica. The results of these calculations are presented in Figure 8(c), where it is evident that the deportment of As to the gas phase $(As)_{gas}$ decreases significantly with an increase of SO_2 because of the reduction of the total gas volume that results from oxygen enrichment. However, arsenic deportment to the slag, $(As)_{slag}$ increases with increasing SO_2 because of the increase of the oxygen partial pressure in the gas, which enhances the oxidation of arsenic to the slag phase. Figure 8(c) also shows that the overall As content of the matte is almost unaffected as the decrease in its removal by volatilization is offset by an increase in the elimination by slagging.

Figure 2 shows that slag basicity has a huge effect on the activity coefficient of $AsO_{1.5}$ in slag, with about two orders of magnitude variation in $\gamma_{AsO_{1.5}}$ as the basicity changes from silica-saturated iron silicate to calcium ferrite slag. Thus, the effect of the $CaO/(CaO + SiO_2)$ ratio in the slag on the arsenic distribution between the phases should be of much interest as it could provide opportunities to improve the management of arsenic in copper smelting and converting. To explore this option further, the model was used to calculate the deportment of As between phases with a varying $CaO/(CaO + SiO_2)$ ratio in the slag at 1523 K (1250 °C), 0.1 atm of SO_2, and a matte grade of 60 pct Cu. The results obtained are shown in Figure 8(d). It can be observed that the portion of the As reporting to the slag increases from 15 pct to 21 pct as the slag basicity increases from 0 to 0.33. Consequently, the As deportment to the gas $(As)_{gas}$ decreases, and the degree of removal of As from the matte increases by increasing the slag basicity. When the $CaO/(CaO + SiO_2)$ ratio in the slag reaches 0.33, solid phases (*e.g.*, spinel) start to precipitate from the liquid slag; however, in the calcium ferrite rich end, such solid phases are less stable and the liquid slag can absorb considerably more As.

Figure 8(e) shows the effect of the arsenic concentration in the feed on the arsenic deportment to the phases. In the range studied, the volatilization of arsenic increases with an increasing level of arsenic in the feed because the arsenic is transferred to the gas phase as AsS, AsO, and As_2. The dependence of the partial pressure of AsS and AsO on the arsenic concentration is linear, whereas the partial pressure of As_2 is dependent on the square of the concentration. As a result, the removal of arsenic as a gaseous As_2 species increases with an increasing arsenic concentration.

The vapor pressure of the arsenic gaseous species increases with an increasing temperature. Therefore, as shown in Figure 8(f), a higher smelting temperature leads to a higher degree of As removal from condensed phases by the gas phase. Figure 8(f) also shows that the deportment of As to the slag decreases with an increasing temperature because the activity coefficient of arsenic oxide increases with an increasing temperature.

These modeling results show that the removal of arsenic by the gas phase is dominant during the copper smelting. Recycling the As-containing dust/fumes through the smelting furnace causes an increase in the As feed in the circuit and results in the As concentration in the anode copper destined for refining. Therefore, the effective collection and safe disposal of the fume/dust would be a significant issue, particularly when high As concentrates are being treated. Alternative practices that lead to bleeding the As from the process flowsheet therefore are necessary.

3. *Copper converting*

To simulate the continuous copper-converting stage, the calculated composition of matte produced from the smelting of the concentrate was used as the starting point for the steady-state converting processes. In most cases, the silica-saturated iron silicate slag was used to investigate the effects of initial matte grade and partial pressure of SO_2 at 1523 K (1250 °C). The results obtained for the As deportment during the conversion

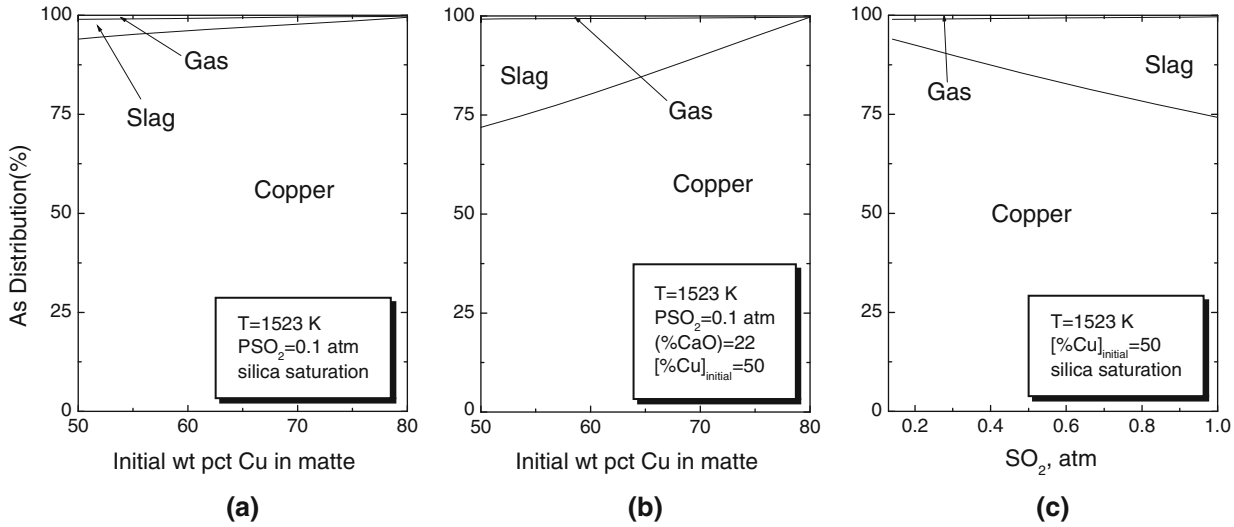

Fig. 9—The distribution of As among the gas, slag, and molten copper phases in continuous converting of copper matte from the smelting stage to blister at 1523 K (1250 °C). (*a*) Silica-saturated iron silicate slag, (*b*) calcium ferrite slag with 22 pct CaO, and (*c*) silica-saturated iron silicate slag.

of copper matte to blister copper with less than 1 wt pct S are presented in Figure 9. Note that in contrast to copper smelting, during converting, liquid copper with a high affinity for As coexists with other phases; thus this blister copper would absorb most As during converting. As shown in Figure 9(a), only 1 pct of As in the starting matte was vaporized when the 50 pct matte grade was converted to blister copper. The deportment of As to the gas and slag phases decreased with an increasing initial matte grade; thus, when iron silicate slag is used for the converting stage, nearly all As reports to the liquid copper phase. When converting with the calcium ferrite slag (Figure 9(b)), about 27 pct of As in the starting matte was removed into the slag when the 50 pct matte grade was converted to blister copper. Figure 9(c) shows the effect of SO_2 partial pressure in the gas during the conversion to be similar to the smelting stage (*i.e.*, the As deportment to the slag phase increases with SO_2 partial pressure because of the increase in oxygen potential). Converting this increase in the As content of the slag translates into a decreasing level of As in the blister copper phase. Thus, oxygen enrichment in the converting stage should result in lower levels of As in the blister copper.

C. *Modeling Batch-Type Operations*

Currently, the Pierce-Smith converter is the most widely used reactor around the world for converting the matte to blister copper. In this case, the converting process can be classified into slag making and copper making stages. In the following sections, the results from modeling these two stages will be presented. Note that the matte and slag temperature changes during the batch-type converting. These changes in temperature have some effect on the As distribution. In this study, the temperature was kept constant during calculation to simplify the process modeling. To represent the As distribution between the slag and the matte during converting, a temperature of 1523 K (1250 °C), which is close to the final point temperature, was used in these model calculation.

1. *Slag making*

During the slag making stage, the FeS in the matte is oxidized to FeO, Fe_2O_3, and SO_2. At the end of slag making, the FeS content of the matte reaches 1 to 2 pct, and white metal (principally Cu_2S) is produced. Usually all slag produced from the slag blow stage is removed, and the white metal then is converted to blister copper (~1 pct S) in the copper making stage. Figures 10(a) and (b) show the calculated results for the deportment of arsenic among the gas, slag, and matte phases at 1523 K (1250 °C) during the course of converting a 50 pct Cu matte grade when iron silicate slag and calcium ferrite slag are used, respectively. When iron silicate slag is produced, (Figure 10(a)), about 73 pct and 7 pct of arsenic were removed *via* volatilization and slagging, respectively. When the calcium ferrite slag is used (Figure 10(b)), As removal *via* the gas and slag were 23 pct and 67 pct, respectively. The overall elimination of arsenic from the matte by using the calcium ferrite slag is 10 pct higher than using the iron silicate slag.

Figure 10(c) shows the effect of the initial matte grade on the deportment of As between phases during the slag making stage. It is evident that a higher initial matte grade results in lower deportment to the gas phase during the slag making stage of converting. This finding is predominantly a result of the reduced volume of air required to convert high-grade mattes. Through considering the results shown in Figures 7(a) and 10(c), smelting of concentrates to the matte with 50 to 60 pct copper followed by the batch-type converting will result in the most effective practice for the overall removal of As from mattes/white metal when the iron silicate slag is practiced.

2. *Copper making*

During the copper making stage, the S in the white metal is oxidized to produce liquid copper (blister) with

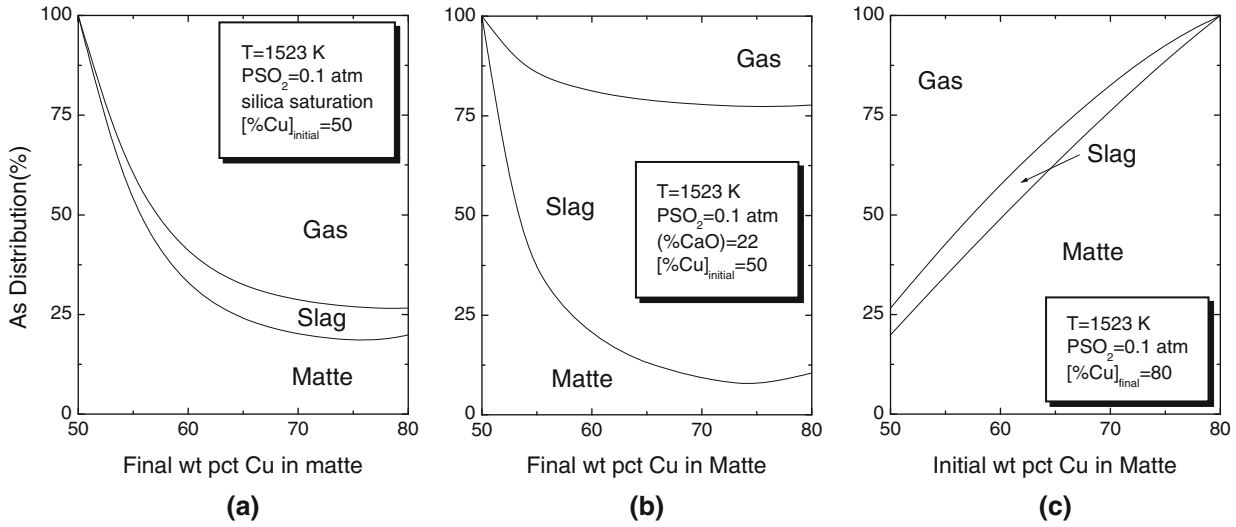

Fig. 10—The distribution of As among the gas, slag, and matte phases during batch-type converting of copper matte from the smelting stage to white metal at 1523 K (1250 °C). (*a*) Silica-saturated iron silicate slag; (*b*) calcium ferrite slag with 22 pct CaO, and (*c*) silica-saturated iron silicate slag.

less than 1 pct S. Because of the miscibility gap between Cu_2S (white metal) and Cu~1 pct S (blister copper), these two phases coexist for most of this converting period. As the arsenic activity coefficient in liquid copper is very low and virtually no slag is present during this stage of copper making, the modeling results show that nearly all arsenic reports to the liquid copper phase.

V. CONCLUSIONS

The thermodynamic data for arsenic in liquid copper, matte, and slag have been reviewed, evaluated, and optimized by using the Redlich-Kister-Muggianu polynomial, quasichemical model, and cell model, respectively. The developed databases have been incorporated into the MPE software developed by CSIRO, which has resulted in an extension of the capability of this software, thus making it a useful tool for modeling the distribution of arsenic among phases under varied operating conditions. This new feature of MPE enables the development of practices for the better management and safe disposal of arsenic.

The distribution of As between the slag and the matte in commercial bath smelting and flash smelting processes was compared with the modeling results. This comparison suggests that commercial processes such as the Noranda process, Mitsubishi process, Isasmelt process, and Outokumpo flash smelting process are approaching equilibrium. Analysis of these data indicates that improvements in the As removal from matte could be achieved by taking appropriate measures to reduce the degree of disequilibrium between the phases as well as by modifying the operating practices to enhance the deportment to the slag and gas phases.

The deportment of arsenic between phases in both continuous copper smelting/converting and batch-type copper-converting processes also were modeled using the MPE software. The results from these simulations show that a high degree of arsenic removal could be achieved through the volatilization of the arsenic-containing species into the gas phase during the smelting stage and the first stage of converting.

The recycling of arsenic-containing dust/fumes, which precipitate from the cooling of off-gas, back into the smelting furnace causes an increased level of arsenic loading in the circuit, thus leading to a higher concentration of As in the anode copper destined for refining. Therefore, an alternative treatment of the dust/fumes to allow for effective bleeding of the arsenic from the circuit and the safe disposal of arsenic fumes is a significant issue, particularly when high arsenic concentrates are being treated.

The replacement of SiO_2 with CaO in the slag increased the solubility of $AsO_{1.5}$ in the slag and therefore increased the degree of arsenic removal through slagging. The modeling results also showed that because of the strong affinity of copper for arsenic, during the converting to blister copper, most arsenic reports to the liquid copper. Thus, the elimination of arsenic should be among the aims of concentrate smelting and the first stage of converting when liquid copper is not present. The modeling results also suggest that the flash smelting of concentrates to the matte with 50 to 60 pct copper followed by the batch-type converting will lead to the most efficient means of arsenic removal.

ACKNOWLEDGMENTS

The authors thank all our sponsors for providing the financial support for this work through the AMIRA International, CSIRO—Minerals Down Under Flagship and Centre for Sustainable Resource Processing. A component of this project was carried out under the auspice and with the financial support of the Centre for

Sustainable Resource Processing, which is established and supported under the Australian Government's Cooperative Research Centres Program.

REFERENCES

1. M. Nagamori and P.C. Chaubal: *Metall. Trans. B*, 1982, vol. 13B, pp. 319–29.
2. K. Itagaki and A. Yazawa: in *Advance in Sulfide Smelting, Vol. 1, Basic Principles*, H.Y. Sohn, D.B. George, and A.D. Zunkel, eds., TMS-AIME, Warrendale, PA, 1983, pp. 119–42.
3. H.G. Kim and H.Y. Sohn: *Trans. Inst. Min. Metall. C*, 1996, vol. 105, pp. C151–63.
4. P. Tan and C. Zhang: *Scand. J. Metall.*, 1997, vol. 26, pp. 115–22.
5. H.L. Lukas, S.G. Fries, and B. Sundman: *Computational Thermodynamics: The CALPHAD Method*, Cambridge University Press, Cambridge, UK, 2007.
6. L. Zhang, S. Jahanshahi, S. Sun, M. Lim, B. Bourke, S. Wright, and M. Somerville: *Mater. Forum*, 2001, vol. 25, pp. 136–53.
7. L. Zhang, S. Jahanshahi, S. Sun, C. Chen, B. Bourke, S. Wright, and M. Somerville: *JOM*, 2002, vol. 54, pp. 51–56.
8. S. Jahanshahi, L. Zhang, S. Sun, D. Langberg, D. Xie, and C. Chen: *VII Int. Conf. on Molten Slags, Fluxes and Salts*, The South African Institute of Mining and Metallurgy, Cape Town, South Africa, 2004, pp. 493–502.
9. C. Chen, L. Zhang, S. Wright, and S. Jahanshahi: *Proc. Sohn Int. Symp.*, F. Kongoli and R.G. Reddy, eds., TMS, Warrendale, PA, 2006, pp. 335–48.
10. Y.M. Muggianu, M. Gambino, and J.P. Bros: *J. Chim. Phys. Phys.-Chim. Biol.*, 1975, vol. 72, pp. 83–88.
11. H. Gaye and J. Welfringer: *Second Int. Symp. on Metallurgical Slags and Fluxes*, TMS-AIME, Warrendale, PA, 1984, pp. 357–75.
12. F. Kongoli, Y. Dessureault, and A.D. Pelton: *Metall. Mater. Trans. B*, 1998, vol. 29B, pp. 591–601.
13. F. Kongoli and A.D. Pelton: *Metall. Trans. B*, 1999, vol. 30B, pp. 443–450.
14. N.A. Gocken: *Bull. Alloy Phase Diagram*, 1989, vol. 10 (1), pp. 11–22.
15. M. Hino, J.M. Toguri, and M. Nagamori: *Can. Metall. Q.*, 1986, vol. 25 (2), pp. 195–97.
16. O. Knacke, O. Kubachewski, and K. Hesselmann: *Thermochemical Properties of Inorganic Substances*, Springer-Verlag, Berlin, Germany, 1991.
17. I. Ansara and B. Sundman: in *Computer Handling and Dissemination of Data*, P.S. Glaser, ed., Elsevier Science Ltd, Atlanta, GA, 1986, pp. 154–58.
18. V.J. Bode, J. Gerlach, and F. Pawlek: *Erzmetall*, 1971, vol. 24, pp. 480–85.
19. T. Azakami and A. Yazawa: *Can. Metall. Q.*, 1976, vol. 15, pp. 111–21.
20. D.G. Jones and D.H. Philipp: *Trans. Inst. Min. Metall. C*, 1979, vol. 88, pp. 7–10.
21. M. Hino and T. Azakami: *Metall. Rev. MMIJ*, 1986, vol. 3, pp. 61–78.
22. M. Hino and J.M. Toguri: *Metall. Trans. B*, 1986, vol. 17B, pp. 755–61.
23. B. Pei: *Scand. J. Metall.*, 1993, vol. 22, pp. 24–29.
24. R.G. Reddy and J.C. Font: *Metall. Mater. Trans. B*, 2003, vol. 34B, pp. 565–71.
25. C. Chen and S. Jahanshahi: *Metall. Mater. Trans. B*, 2010, vol. 41B. Doi:10.1007/s11663-010-9430-0.
26. Y. Takeda, S. Ishiwata, and A. Yazawa: *Trans. Jpn. Inst. Met.*, 1983, vol. 24, pp. 518–28.
27. M. Kashima, M. Eguchi, and A. Yazawa: *Trans. Jpn. Inst. Met.*, 1978, vol. 19, pp. 152–58.
28. G. Roghani, Y. Takeda, and K. Itagaki: *Metall. Mater. Trans. B*, 2000, vol. 31B, pp. 705–12.
29. N. Asano and M. Wada: *Suiyokaishi*, 1968, vol. 16, pp. 385–8.
30. M. Nagamori, P.J. Mackey, and P. Tarassoff: *Metall. Trans. B*, 1975, vol. 6B, pp. 295–301.
31. D.G. Mendoza, M. Hino, and K. Itagaki: *Metall. Mater. Trans.*, 2001, vol. 42, pp. 2427–33.
32. K. Itagaki, M. Hino, and A. Yazawa: *Erzmetal*, 1983, vol. 36, pp. 59–64.
33. K.H. Lau, R.H. Lamoreaux, and D.L. Hildenbrand: *Metall. Trans. B*, 1983, vol. 14B, pp. 253–58.
34. A. Roine and H. Jalkanen: *Metall. Trans. B.*, 1985, vol. 16B, pp. 129–40.
35. T. Zhong and D.C. Lynch: *Metall. Mater. Trans. B*, 2001, vol. 32B, pp. 437–47.
36. A. Yazawa, S. Nakazawa, and Y. Takeda: in *Advances in Sulfide Smelting, Vol. 1, Basic Principles*, H.Y. Sohn, D.B. George, and A.D. Zunkel, eds., TMS-AIME, Warrendale, PA, 1983, pp. 99–117.
37. E.A. Johnson, L.L. Oden, P.E. Sanker, and R.L. Fulton: Bureau of Mines Report of Investigations, No. 8874, U.S. Dept. of the Interior, Bureau of Mines, 1984, pp. 1–9.
38. E. Ohshima and M. Hayashi: *Metall. Rev. MMIJ*, 1986, vol. 3 (3), pp. 113–29.
39. C. Acuna and A. Yazawa: *Trans. Jpn. Inst. Met.*, 1987, vol. 28, pp. 498–506.
40. G. Roghani, J.C. Font, M. Hino, and K. Itagaki: *Trans. Jpn. Inst. Met.*, 1996, vol. 37, pp. 1574–9.
41. H. Persson, M. Iwanic, S. El-Barnachawy, and P.J. Mackey: *JOM*, 1986, vol. 9, pp. 34–37.
42. C.R. Fountain, M.D. Coulter, and J.S. Edwards: *Copper 91-Cobre 91 Int. Conf. Volume IV-Pyrometallurgy of Copper*, 1991, pp. 360–371.
43. P. Taskinen, K. Seppala, J. Laulumaa, and J. Poijarvi: *Trans. Inst. Min. Metall. C*, 2001, vol. 110, pp. C94–100.
44. Z. Yuan: *Copper99-Cobre99, Vol. V-Smelting Operations and Advances*, TMS, Warrendale, PA, 1999, pp. 345–55.